A NUMERICAL MODEL FOR THE 29-STRAND NET BRAID

E.M.J Niessen, L.J.M van de Klundert
University of Twente, Dept. of Applied Physics
P.O. Box 217, 7500 AE Enschede, The Netherlands

Abstract

A discrete modeling technique is used to analyze the 29-strand NET braid in changing magnetic fields. Input for the model is the $V-I$ relation of an individual strand and the contact resistance between touching strands. The model gives 3 dimensional current patterns, $V-I$ relations and corresponding energy losses for the cable. The analysis shows a strong dependence of the cable properties on the direction of the field.

Introduction

Properties of a superconducting cable are modeled by representing the cable as a network of node points[1]. Between two node points either flows a superconducting parallel current in a strand or a contact current between two touching strands. Kirchhoff's equations can be applied to the node points and the resulting meshes. The meshes incorporate the induced voltage due to applied magnetic field changes. Basic elements of the model are the $V-I$ relation of a single strand and the contact resistance between these strands.

Application of this, so called, network method was reported for simple cable geometries, *e.g.* a superconducting composite[2], a round twisted cable and a Rutherford cable[1,3]. The complicated geometry of the 29-strand NET braid, caused by the special braiding technique developed by ABB, is modeled. The positions of the contact currents depend strongly on this braiding technique.

Geometry of the cable

We will explain the geometry of an idealized cable which is in good agreement with a realistic cable. The 29-strand NET braid has a cabling length L_c of 460 mm. Every $460/29 \approx 16$ mm the structure of a cross-section of the cable is repeated. This periodic length can again be divided into four equal parts of 4 mm. When we project the positions of the strands of the cable on the cross-sectional plane 4x29 = 116 positions should occur. However, due to the crossing of the strands some positions will occur twice, and 97 points are left. These 97 points are shown in Figure 1. The letters A, B, C and D refer to the positions in the four subsequent planes. Here also the x, y and z-direction are defined and the thickness d of a strand is shown. The 19 points marked E belong to both the A and C plane. In this figure we can track the subsequent positions of one strand in one cabling length by following the letters A or E, B, C or E, D, A or E, B, ... Recognize that these subsequent positions follow a complicated pattern in the cross-sectional plane. Note that in the A and C plane the strands do not touch each other at all, whereas some do in the B and D plane. Defining all the contacts in the planes B and D is a good approximation for the realistic cable.

Manuscript received September 24, 1990.

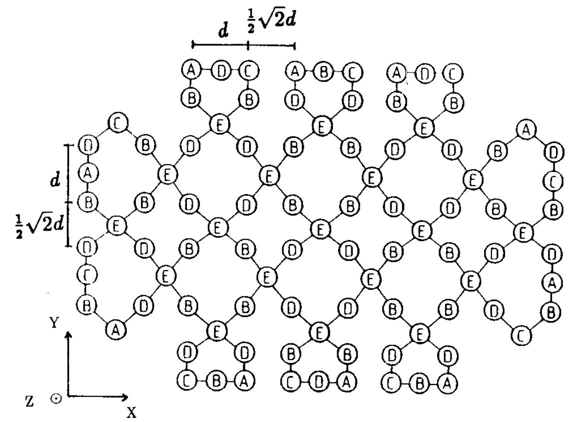

Figure 1: Positions of the strands at four equidistant planes subdividing one period of the braid. For A to E see text.

The model

In this section we define the currents in the model. One cabling length L_c of the braid can be divided in 29 periods, each consisting of 2 layers. Layer 1 consists of a plane in which the strands do not touch (plane A) and a plane in which some strands can touch (plane B). For layer 2 they are plane C and D respectively. The positions of the strands in plane B and D for both layers are shown in Figures 2 and 3 respectively.

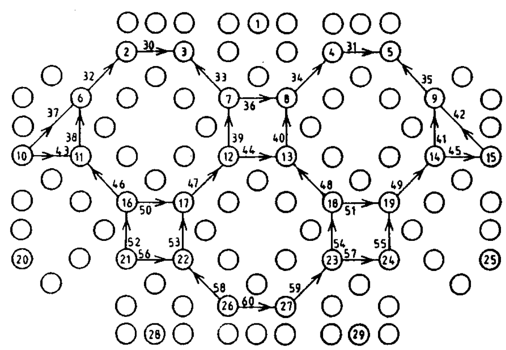

Figure 2: Definition of the parallel and contact currents in plane B of Figure 1.

In these planes strands can touch each other, which causes contact currents to flow between these strands. In Figures 2 and 3 also the numbers of the parallel and contact currents in two subsequent layers are defined. Here the parallel currents are defined to flow in the positive z-direction and the contact currents flow in the direction given by the arrow. In one layer we see 29 parallel and 31 contact currents. The parallel currents are defined in the non-touching planes A and C, while the contact currents are defined in the touching planes B and D. This means that we have a network of node points connected by defined currents. In the calculations current I_{10} and I_{15} have a y-coordinate $d/2$ greater and current I_{75} and I_{80} have a y-coordinate $d/2$ smaller than shown in Figure 2 and 3.

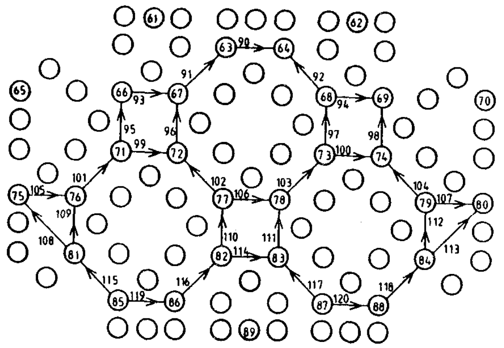

Figure 3: Definition of the parallel and contact currents in plane D of Figure 1.

In one period there are 120 unknown currents. In a piece of the braid of M periods, $120M(=N)$ unknowns must be determined.

Equations

For solving the currents we use Kirchhoff's equations together with a supplementary set of constitutive equations. We only consider time independent currents and do not take the induced field due to the currents themselves into account. Kirchhoff's equations read:

$$\sum_h I_h = 0, \tag{1}$$

$$\sum_i V_i = -V^{ind}. \tag{2}$$

Eq.(1) is valid in each node point of the network. Index h contains all the current numbers connected to a specific node point. Eq.(2) has a right hand side $-V^{ind}$, the flux change pointing through the surface of a mesh. Index i contains all the voltage numbers in that specific mesh.
Once per period one has to add:

$$\sum_j I_j = I_0, \tag{3}$$

stating that all currents pointing through some cross-section of the cable add up to the applied transport current I_0. The I_h's of (1) and the V_i's of (2) are connected through the constitutive equations. These equations can take three forms denoted by the indices n, u and s respectively[1]:

- normal contact current:

$$V_n = R_k I_n \tag{4}$$

- unsaturated superconducting current if $|V_u| \leq V_0$:

$$V_u = \frac{V_0 R_p}{I_c R_p + V_0} I_u \equiv R_q I_u \tag{5}$$

- saturated superconducting current if $|V_s| > V_0$:

$$V_s = R_p (I_s - I_c \mathrm{sign}(V_s)). \tag{6}$$

In eq.(4-6) R_k is the contact resistance, R_p is the parallel resistance of the normal conducting part of a strand element, R_q is the effective resistance of a strand element in the unsaturated case, I_c is the threshold value of the saturation in a composite superconducting strand, depending on its inner structure[1], V_0 is the voltage across a strand element in case the element is just saturated ($V_0 = 8(0.460/58)R_f|\dot{B}_\perp|/3\pi$), R_f is the radius of the superconducting filaments in a strand and $\dot{B}_\perp$ is the time derivative of the perpendicular component of the applied magnetic field. Substitution of (4-6) in (2) yields:

$$\sum_n R_k I_n + \sum_u R_q I_u + \sum_s R_p I_s = -V^{ind} + \sum_s R_p I_c \mathrm{sign}(V_s). \tag{7}$$

Eqs.(1), (3) and (7) are used for the calculation of the parallel and contact currents. In one period we use 57 times eq.(1), once eq.(3) and 62 times eq.(7) for independent meshes. It is possible to minimize the maximal mesh length to three layers. We assume periodic boundary conditions over the total of M periods. Because the maximal mesh length is 3 layers, these conditions are used *only* in the last period: for solving the currents in period M we need currents in period $M+1$. These are set equal to the currents in period 1.
In the mesh equations the contact resistances satisfy eq.(4) while the parallel resistances R_s satisfy eq.(5) or (6). The non-linearity in R_s results in an iterative solving method. We assume the value of R_s and the sign of V_s, and check the validity of the requirements on the resulting V_u and V_s. For convergence the same restrictions can be used as described by Hartmann[4], where it was shown that one should not allow a strand element to change from a negative saturation into a positive one or vice versa, but only allow saturated elements to turn in unsaturated ones or vice versa.
Recognize that the critical current I_c can be taken to be $\dot{B}_\perp$ dependent[1]. This case is not considered here, because our first interest is to investigate the influence of the braiding technique on cable properties.

Reduction technique

Considering the numbering of the currents, it is possible for this model to create a sparse and upper matrix, except for those equations in which the boundary conditions are included: the last period of the cable. The principal diagonal of this matrix is non-zero. We use equation i of the matrix, with $i \in [1, N-120]$, for eliminating variable I_i out of equation j, with $j \in [N-119, N]$. This results in a 120x120 full matrix for currents N-119 to N (we *prescribe* the pivoting element for the elimination to be the *principal* diagonal). Solving the relatively small matrix gives the currents in the last period. Back substitution in equation N-120 to 1 renders the whole solution.

This technique gives an accurate solution because we use good pivots in the reduction of the matrix (for the mesh equations the principal diagonal R_k is dominant in comparison to R_s) and a full pivoting matrix solver for the 120x120 matrix.
The operations for obtaining the whole solution can be divided into two parts:
1: the reduction: the mean number of non-zero coefficients in a row is $\alpha = 5.4$. We eliminate N-120 variables from 120 equations.
2: full pivoting matrix solving: it uses $O(120^3)$ operations.
The number of operations of the first step is *linear* proportional to the number of unknowns N whereas the second does not depend on N. The technique reduces the CPU time of the program considerably in comparison to other sparse solvers.

Infinite periodic cables

In this section we consider a cable with length L, consisting of M periods in an applied magnetic field $\dot{B}$ in the x or y direction. The voltage across the cable per unit length is given by:

$$V/l = \frac{1}{29L}\sum_{i=1}^{M}\left\{\sum_{j=1}^{29} V_{i,j} + \sum_{j=61}^{89} V_{i,j}\right\}, \qquad (8)$$

with $V_{i,j}$ is the voltage difference across a strand element j in period i. The parallel and contact losses per cable volume are:

$$P_{par}/\vartheta = \frac{1}{\vartheta}\sum_{i=1}^{M}\left\{\sum_{j=1}^{29} I_{i,j}V_{i,j} + \sum_{j=61}^{89} I_{i,j}V_{i,j}\right\}, \qquad (9)$$

$$P_k/\vartheta = \frac{1}{\vartheta}\sum_{i=1}^{M}\left\{\sum_{j=30}^{60} I_{i,j}V_{i,j} + \sum_{j=90}^{120} I_{i,j}V_{i,j}\right\}, \qquad (10)$$

with $I_{i,j}$ current number j in period i and the cable volume $\vartheta = 29\pi(\frac{1}{2}d)^2 L$.
For the *unsaturated case* $R_s \ll R_k$ which gives:

$$V/l = c_1\frac{I_0 R_f \dot{B}}{I_c}\,[V/m], \qquad (11)$$

$$P_{par}/\vartheta = c_2\frac{I_0^2 R_f \dot{B}}{I_c d^2} + c_3\frac{R_f \dot{B}^3 L_c^2}{I_c R_k^2}\,[W/m^3], \qquad (12)$$

$$P_k/\vartheta = c_4\frac{\dot{B}^2 L_c}{R_k}\,[W/m^3], \qquad (13)$$

for $R_s = V_0/I_c$ (as $R_p \gg V_0/I_c$). Some of the constants c in the above expressions depend on the direction of the field. This is denoted by the extra subscript 'x' and 'y' for a $\dot{B}_x$ and $\dot{B}_y$ field respectively. The numerical calculated constants are: $c_{1x} = c_{1y} = 2.93\ 10^{-2}$, $c_{2x} = c_{2y} = 1.29\ 10^{-3}$ and

$$c_{3x} = 3.53\ 10^{-3};\quad c_{3y} = 5.32\ 10^{-3};$$
$$c_{4x} = 1.84;\quad c_{4y} = 6.01.$$

For a magnetic field in the z-direction we only give P_k/ϑ for $I_0 = 0$:

$$P_{k,z}/\vartheta = 5.08\ 10^2\ \frac{\dot{B}_z^2 d^2}{R_k L_c}\,[W/m^3]. \qquad (14)$$

For the *saturated case* R_s is given by eq.(6), resulting in:

$$V/l = \frac{58 R_p I_c}{L_c}\left(\frac{I_0}{29 I_c} - 1\right)\,[V/m] \qquad (15)$$

$$\text{and } P_{par}/\vartheta = \frac{I_0}{29\pi d^2/4} V/l\,[W/m^3]. \qquad (16)$$

These two expressions are valid for both a $\dot{B}_x$ and $\dot{B}_y$ field for we neglected the induced losses. For the contact loss we get:

$$P_k/\vartheta = \frac{\dot{B}^2 L_c}{R_k}F\,[W/m^3]. \qquad (17)$$

Here F is a polynomial in R_k and R_p with coefficients depending on the direction of the field. We consider three cases:

$R_k \gg R_p$: $F_x = c_{4x}$; $F_y = c_{4y}$;
$R_k = R_p$: $F_x = 2.69\ 10^{-3}$; $F_y = 2.02\ 10^{-3}$;
$R_k \ll R_p$: $F_x = 3.71\ 10^{-3}\ R_k^2/R_p^2$; $F_y = 4.31\ 10^{-3}\ R_k^2/R_p^2$.

The *partly saturated case* will be analyzed numerically. When we start with a partly saturated configuration and R_k decreases, V^{ind} will induce greater currents in a mesh, which means that S, the relative number of saturated strand elements with respect to all strand elements, increases. Also P_{par} and P_k increase. When R_p increases the resulting voltage will increase, because the cable has to carry a transport current I_0: S and P_{par} increase. P_k decreases as the higher resistances in a mesh decrease the induced currents. When R_f decreases S increases. The employed parameter set is: $R_k = 10^{-3}\ \Omega$, $R_p = 10^{-5}\ \Omega$, $R_f = 10^{-5}\ m$, $I_c = 500\ A$ and $d = 10^{-3}\ m$. V/l, S and P_k/ϑ are given as function of I_0 for three values of $\dot{B}_x$ in Figure 4.

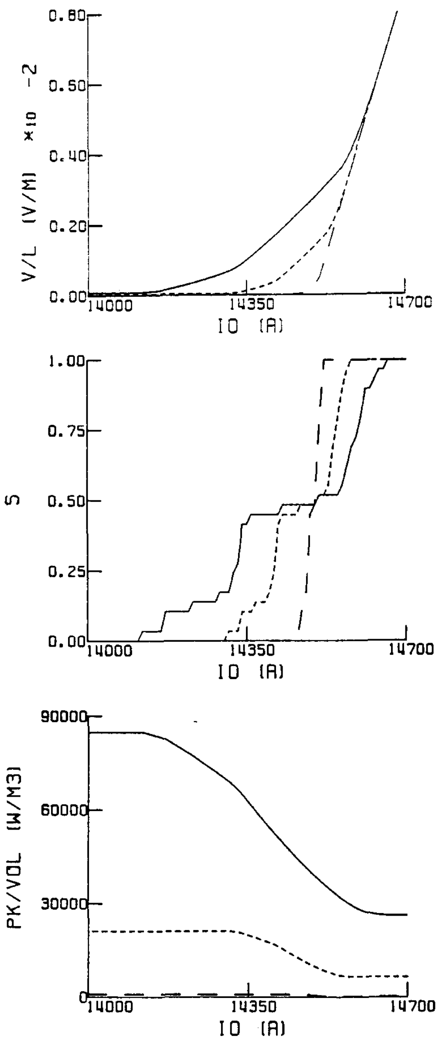

Figure 4: V/l, S and P_k/ϑ of the cable as function of I_0. The lines (——), (- - -) and (— —) correspond to $\dot{B}_x = 10$, 5 and 1 T/s respectively.

The transition from an unsaturated to a completely saturated cable is given. Observe that V/l consists of several, almost straight lines. Along such a line S increases slowly, while at a change between two straight lines S increases fast. We also see that due to the saturation P_k decreases.
The saturation process described in the paragraph above is visualized in Figure 5.

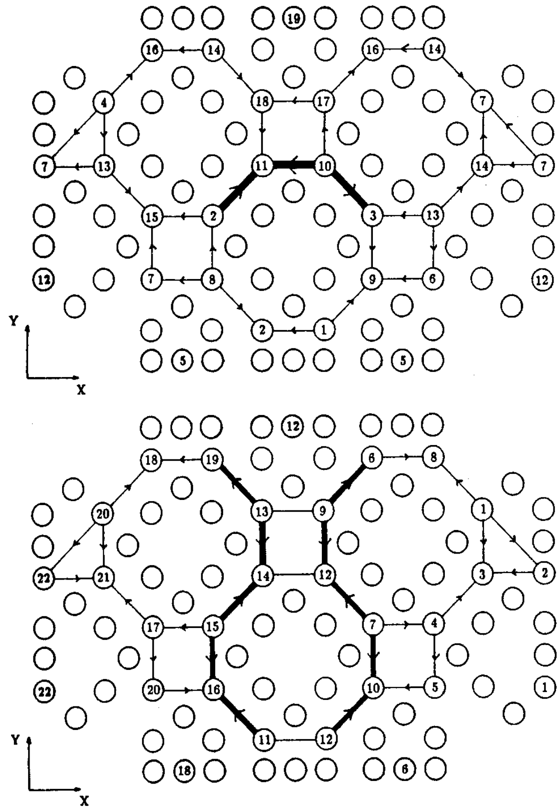

Figure 5: Saturation process in a $\dot{B}_x$ and $\dot{B}_y$ field (upper/lower figure) of 1 T/s for increasing I_0. For the numbers see text.

It indicates the order in which the strands become saturated as I_0 increases from zero to its maximal value. In the upper and lower part we see the order for a $\dot{B}_x$ and $\dot{B}_y$ field of 1 T/s respectively. For $I_0 = 0$ no saturation occurs. A higher number in the figure means that the strand saturates for a greater value of I_0. The arrows give the direction of the contact currents in case all the strands are saturated. The most important contact currents are indicated with a thick arrow: the absolute value of these contact currents is greater than 75% of the greatest contact current for that specific $\dot{B}$ field. We see that for the $\dot{B}_y$ field the contact currents are zero in the symmetrical line parallel to the y-axis in the middle of the cable, which is to be expected. Note that for a $\dot{B}_y$ field the number of important contact currents is much greater than for a $\dot{B}_x$ field.

Cables of finite length

Now we consider a *finite* piece of the braid with length L placed in an applied magnetic field $B(t) = \dot{B}t$ with $\dot{B}$ constant. We investigate the steady state current distribution in the cable assuming that no saturation occurs. Due to the finite length of the cable the parallel currents at either end of the cable vanish. The resulting contact losses, scaled on their maximum are given as a function of L/L_c for a $\dot{B}_x, \dot{B}_y$ and $\dot{B}_z$ field in Figure 6. As reference the scaled contact loss power density p for a hollow, twisted cable is shown[4,5], with the twistlength L_p equal L_c:

$$p = 1 - \left(\frac{L_c}{\pi L}\right)^2 \sin^2\left(\frac{\pi L}{L_c}\right), \qquad (18)$$

$P_{k,x}$ displays an oscillatory behaviour as a function of L/L_c as does a twisted cable. $P_{k,y}$ oscillates with the double frequency $L/2L_c$. This doubling is caused by the symmetry of the model with respect to the centre line of the braid parallel to the y-axis. On this symmetrical axis the contact currents are equal to zero. The parallel currents crossing this line are not zero. $P_{k,z}$ is almost constant for $L > L_c$.

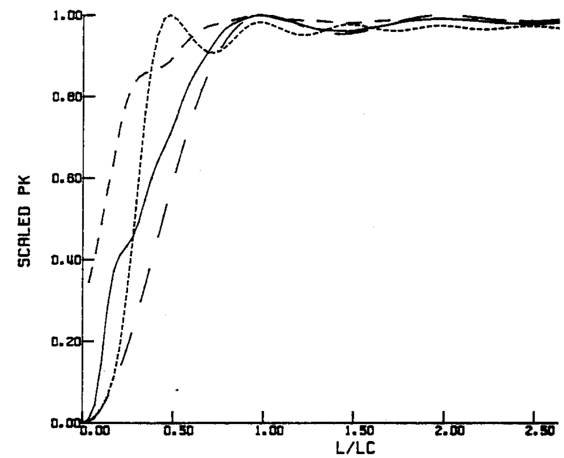

Figure 6: Scaled value of the contact losses as function of L/L_c. The lines (——), (- - -), (— —) and (—— ——) correspond to a $\dot{B}_x, \dot{B}_y$ and $\dot{B}_z$ field on the braid and a $\dot{B}_\perp$ field on the hollow twist, respectively.

References

1. E.M.J. Niessen, D. ter Avest and L.J.M. van de Klundert, "Application of the network method to superconducting cables", *Proc. LTEC90*, July 1990, pp 5.4.
2. D. Ciazynski and B. Turck, "Theoretical and experimental study of the saturation of a superconducting composite under fast changing magnetic field", *Cryogenics* 24, Oct. 1984, pp 507-514.
3. V.E. Sytnikov et al., "Coupling losses in superconducting transposed conductors located in changing magnetic fields", *Cryogenics* 29, Sept. 1989, pp 926-930.
4. R.A. Hartmann, "A contribution to the understanding of AC losses in composite superconductors", *thesis* University of Twente, Enschede, 1989.
5. G. Ries and S. Takács, "Coupling losses in finite length of superconducting cables and in long cables partially in magnetic field", *IEEE Transactions on Magnets* 17, no. 5, 1981, pp 2281-2284.